nature energy

ARTICLES

PUBLISHED: 3 APRIL 2017 | VOLUME: 2 | ARTICLE NUMBER: 17035

Enhancing ionic conductivity in composite polymer electrolytes with well-aligned ceramic nanowires

Wei Liu[1], Seok Woo Lee[2], Dingchang Lin[1], Feifei Shi[1], Shuang Wang[3], Austin D. Sendek[4] and Yi Cui[1,5]*

In contrast to conventional organic liquid electrolytes that have leakage, flammability and chemical stability issues, solid electrolytes are widely considered as a promising candidate for the development of next-generation safe lithium-ion batteries. In solid polymer electrolytes that contain polymers and lithium salts, inorganic nanoparticles are often used as fillers to improve electrochemical performance, structure stability, and mechanical strength. However, such composite polymer electrolytes generally have low ionic conductivity. Here we report that a composite polymer electrolyte with well-aligned inorganic Li^+-conductive nanowires exhibits an ionic conductivity of 6.05×10^{-5} S cm^{-1} at 30 °C, which is one order of magnitude higher than previous polymer electrolytes with randomly aligned nanowires. The large conductivity enhancement is ascribed to a fast ion-conducting pathway without crossing junctions on the surfaces of the aligned nanowires. Moreover, the long-term structural stability of the polymer electrolyte is also improved by the use of nanowires.

Considerable effort has been dedicated to improving current rechargeable lithium-ion batteries (LIBs) and to developing new materials, owing to the ever-increasing demand for high-performing, safe and economical energy storage for various applications[1–6]. An exciting research direction is in solid Li-ion electrolyte, which has a large electrochemical stability window and improved safety in comparison to conventional liquid electrolyte with leakage, flammability and poor chemical stability issues. In addition, solid electrolyte can offer one of the most promising approaches to suppress Li metal dendrites to enable the 'holy grail' of high-energy lithium metal batteries. However, using solid Li-ion electrolytes results in lower capacity utilization and deterioration in battery performance, due to the limited ionic conductivity, which remains the principal material challenge[7–10].

Solid Li-ion electrolyte includes two general classes of materials: inorganic materials and organic polymers[1,10]. Among the inorganic electrolytes, those based on sulfides, such as $Li_7P_3S_{11}$ (refs 11,12) and $Li_{10}GeP_2S_{12}$ (ref. 13), show extremely high ionic conductivities ($>10^{-3}$ S cm^{-1} at room temperature). But, the sulfides are very sensitive to O_2 or H_2O. Oxide-based solid electrolytes, such as $Li_{3x}La_{2/3-x}\square_{1/3-2x}TiO_3$ (□ indicates vacancies)[14] and phosphate-based $Li_{1+x}Al_xGe_{2-x}(PO_4)_3$ (ref. 15), have been of great interest owing to their good performance in terms of high ionic conductivity (10^{-4} S cm^{-1}) and good stability with respect to moisture, although their ionic conductivity still needs to be improved. Low-cost processing of inorganic electrolyte also remains to be developed. In contrast, solid polymer electrolytes (SPEs, combination of polymer and lithium salt) can offer shape versatility, flexibility, light weight and low-cost processing. SPEs based on poly(ethylene oxide) (PEO) and polyacrylonitrile (PAN) usually show a low ionic conductivity of 10^{-5}–10^{-7} S cm^{-1} at room temperature, which limits their practical applications[2,16,17]. Moreover, the poor long-term stability of SPEs due to the structural reorganization of polymer chains is also a critical issue[18,19]. Compared with PEO, PAN is thermally more stable[20].

Extensive study has been focused on incorporating inorganic nanofillers into polymer hosts that could combine the advantages of both inorganic electrolytes and organic electrolytes[17,21–27] since the first report on SPEs with α-Al_2O_3 filler by Weston and Steele[28]. It is commonly recognized that the conductivity enhancement by the addition of ceramic nanoparticles is mainly attributed to a reduced crystallinity of the polymer host[29], although the pioneers Wieczorek *et al.*[25,26] and other groups[30–35] suggested an active role of the surface groups of the ceramic nanoparticles in promoting local structural modifications, resulting in an increase in the free Li-ion concentration that can move fast throughout the conductive pathways at the ceramic extended surface. Furthermore, Scrosati *et al.*[36] demonstrated that the nanosized ceramic fillers had an influence on the structural reorganization of polymer chains, with improvement in the long-term structural stability. In our own work[37], we demonstrated that composite polymer electrolytes with randomly dispersed Li^+-conductive nanowires exhibit a significant enhancement of ionic conductivity compared with filler-free electrolytes and nanoparticle-filled electrolytes (Fig. 1a,b).

In the current work we report that compared with random-oriented nanowires, aligned nanowires along the normal direction of electrodes in polymer electrolyte result in one order of magnitude enhancement in ionic conductivity, due to the fast ion conduction on nanowire surfaces without crossing junctions (Fig. 1c). The surface conductivity of the nanowires in polymer electrolyte is calculated to be comparable to the ionic conductivity of liquid electrolyte. In addition, the long-term stability of the polymer electrolytes is also improved by using nanowires.

[1]Department of Materials Science and Engineering, Stanford University, Stanford, California 94305, USA. [2]Geballe Laboratory for Advanced Materials, Stanford University, Stanford, California 94305, USA. [3]Department of Electrical Engineering, Stanford University, Stanford, California 94305, USA. [4]Department of Applied Physics, Stanford University, Stanford, California 94305, USA. [5]Stanford Institute for Materials and Energy Sciences, SLAC National Accelerator Laboratory, 2575 Sand Hill Road, Menlo Park, California 94025, USA. *e-mail: yicui@stanford.edu

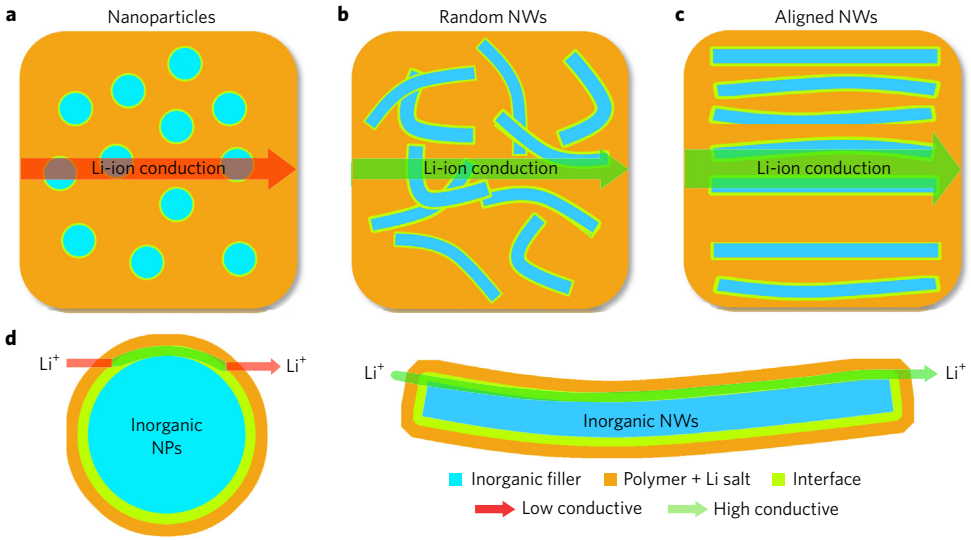

Figure 1 | The comparison of possible Li-ion conduction pathways. a–c, Li-ion conduction pathways in composite polymer electrolytes with nanoparticles (**a**), random nanowires (**b**) and aligned nanowires (**c**). Compared with isolated nanoparticles, random nanowires could supply a more continuous fast conduction pathway for Li ion. Compared with random nanowires, aligned nanowires are free of crossing junctions. **d**, The surface region of inorganic nanoparticles (NPs) and nanowires (NWs) acts as an expressway for Li-ion conduction.

Materials fabrication and characterization

The schematic illustration shown in Fig. 2a indicates the procedure to prepare the PAN-based electrolyte with well-oriented $Li_{0.33}La_{0.557}TiO_3$ (LLTO) nanowires. The interdigital Pt electrodes on a quartz substrate across an area of 10 × 5 mm displayed in Fig. 2b were first fabricated by means of lithography. The width of the Pt electrodes is 20 or 40 μm and the gap between two stripes is 20 μm. To obtain well-aligned nanowires by electrospinning, a grounded drum rotating at 6,000 r.p.m. was used as the collector. The interdigital Pt electrodes were placed on the drum at controlled angles during electrospinning. The angles between the elongated direction of the nanowires and the normal direction of the Pt electrodes are 0°, 45° and 90°, respectively. The collection time during electrospinning was controlled precisely to obtain a sufficient (but not excessive) number (about 2,000) of aligned nanowires on the substrate. The as-spun fibres were then calcined at 800 °C in air for 2 h. Subsequently, a dimethylformamide (DMF) solution containing PAN and $LiClO_4$ was cast with a doctor blade on the substrate. Finally, the solid composite electrolytes were obtained by further drying in vacuum and then in a glove box.

To elucidate the complex formation and the elimination of solvent in the electrolytes, measurements of Fourier transform infrared (FTIR) transmittance spectra (Supplementary Fig. 1), differential thermal analysis/thermo-gravimetric (DTA/TG) (Supplementary Fig. 2) and C 1*s* X-ray photoelectron spectroscopy (XPS) core level spectra (Supplementary Fig. 3) were performed. The results indicated that DMF in the PAN-based polymer electrolyte is difficult to completely remove (for details see Supplementary Note 1), due to its fairly high boiling point of 150 °C and its strong affinity with the nitrile group of PAN[38,39], as observed in the reported results. It should be noted that the composite polymer electrolytes and filler-free electrolyte followed strictly the same preparation procedures, which means that their electrical properties are comparable.

The transmission electron microscope (TEM) image in Fig. 2c illustrates that the polycrystalline nanowires with a large aspect ratio show average diameters of 138 nm. The detailed investigation into the micromorphology and phase structure of the nanowires has been systemically reported in our previous work[37]. The nanowires are consistently well aligned and can cover large areas of the electrodes. Together with optical photos (Supplementary Fig. 4a–c), scanning electron microscope (SEM) images of the well-aligned nanowires on the electrodes shown in Fig. 2d–f indicate the orientation angles are 0°± 5°, 45°± 9° and 90°± 8°, respectively. The average spacing between nanowires is about 5 μm. The surface of composite polymer electrolyte with a thickness of 645 nm was smooth and flat, and the nanowires were well embedded in the polymer matrix, as shown in Supplementary Fig. 4d.

Ionic conductivity of composite polymer electrolytes

The ionic conductivities of SPEs were investigated via a.c.-impedance spectroscopy measurements. With well-fitted spectra, typical Nyquist plots for the composite polymer electrolyte with LLTO nanowires at 0° orientation measured at various temperatures are given in Fig. 3a. The inset figure indicates the equivalent circuit used to fit the plots. The semicircle at high and intermediate frequencies is ascribed to the parallel combination of bulk resistance and bulk capacitance. The spike at low frequencies corresponds to the double-layer capacitance formed at the interface between electrode and electrolyte.

The ionic conductivity for composite polymer electrolytes with LLTO nanowires of various orientation angles as a function of temperature is shown in Fig. 3b, together with the data for the electrolytes with randomly dispersed nanowires and with LLTO nanoparticles and the filler-free electrolyte. It should be noted that the weight concentration for the fillers in all these composite polymer electrolytes is 3%. The ionic conductivity of the filler-free polymer electrolyte is 3.62×10^{-7} S cm^{-1} at 30 °C, which is improved to 1.02×10^{-6} S cm^{-1} by adding nanoparticles, and is further increased to 5.40×10^{-6} S cm^{-1} by the incorporation of randomly dispersed nanowires. Hence, the advantage of nanowires with high aspect ratio over isolated nanoparticles can be seen. Furthermore, by replacing the disorderly nanowires with well-aligned nanowires (orientation angle at 0°) in the polymer matrix creates another order of magnitude enhancement in the conductivity (6.05×10^{-5} S cm^{-1}). Accordingly, the hypothesis that aligned nanowires could further improve the conductivity over the random nanowires in composite polymer electrolytes is validated. The aligned nanowires are free of crossing junctions that formed in aggregated nanoparticles or random nanowires with wire-to-wire junctions. In addition, d.c. conductivity data could be converted from the conductivity–frequency dependence plots obtained from impedance spectra[40,41]. The d.c. conductivities of the filler-free electrolyte, the composite electrolyte

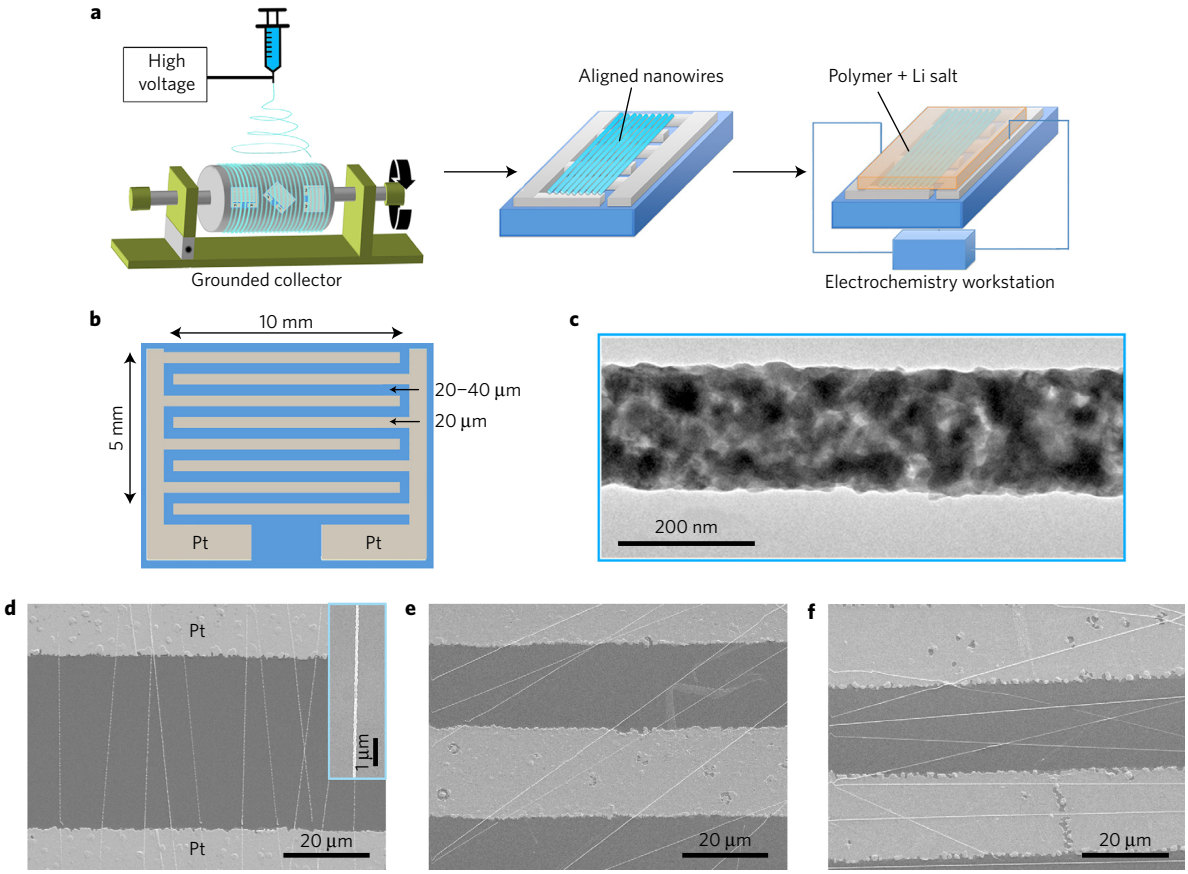

Figure 2 | Synthesis procedure and morphologies for the composite polymer electrolyte with aligned nanowires. a, Synthesis procedure for the composite polymer electrolyte with aligned nanowires together with illustration of the electrode configuration for the a.c.-impedance spectroscopy measurement. The quartz substrates with Pt electrodes are placed at three different orientations on the rotating drum collector during electrospinning. **b**, Interdigital Pt electrode. **c**, TEM images of the LLTO nanowire calcined at 800 °C. **d**–**f**, SEM images of the aligned nanowires at orientations of 0 ° (**d**), 45 ° (**e**) and 90 ° (**f**). The inset in figure **d** is a SEM image at high magnification for the aligned nanowires.

with randomly dispersed nanowires and the electrolyte with aligned nanowires (orientation angle 0°) are 4.31×10^{-7}, 7.82×10^{-6} and 5.02×10^{-5} S cm^{-1} at 30 °C, respectively, which are consistent with the conductivity values obtained from the Nyquist plots.

It is also worth noting from Fig. 3b that the ionic conductivity changes with the angle of the nanowires in these composite electrolytes. For the case of nanowires at 90°, the conductivity is very low (similar to the polymer without filler) at only 1.78×10^{-7} S cm^{-1} at 30 °C, since the long axis of nanowires is parallel to the electrode direction and the surface area of the nanowires does not really cross between the electrodes. For the case of the nanowires at 45°, the conductivity is 2.24×10^{-5} S cm^{-1} at 30 °C, which is lower than for nanowires at 0°. This is because that the continuous length of nanowires across the electrodes for nanowires at 45° is 1.4 times longer than those at 0°. Note that the absolute value of ionic conductivity for the composite electrolytes with aligned nanowires is still not high enough to meet the requirement of ~10^{-3} S cm^{-1}. This is because the nanowire content in the polymer is only ~3.0 wt%. We expect that the ionic conductivity of composite polymer electrolytes with aligned nanowires could be enhanced in the future when a synthesis method with higher nanowire loading is developed. Moreover, it indicated that composite polymer electrolytes with the nanowires showed improved long-term stability compared with the filler-free electrolyte. For details, see Supplementary Note 2.

The nature of the conductivity in SPEs, and in particular whether or not it is cationic conduction, is of significant importance with respect to their potential applications. To clarify the electronic conductivity in the electrolyte, d.c. Hebb–Wagner polarization measurements were performed[42,43]. The sample was sandwiched by an ion-blocking electrode (Au) and a reversible electrode (Li). When a d.c. voltage was applied through the cell, only electronic charge carriers (electrons and holes) can flow through the cell. Supplementary Fig. 8 presents the steady-state current i as a function of the applied voltage. The electronic conductivity could be determined using the equation:

$$i = \frac{kT}{qL}\left[\sigma_e\left(\exp\left(-\frac{Uq}{kT}\right)-1\right)+\sigma_h\left(1-\exp\left(\frac{Uq}{kT}\right)\right)\right] \quad (1)$$

where k, T, q, L and U are the Boltzmann constant, absolute temperature, elementary charge, distance between the electrodes and applied voltage, respectively. The total electronic conductivities ($\sigma_e + \sigma_h$) of the filler-free polymer electrolyte and the composite electrolyte with nanowires are 7.29×10^{-11} and 2.90×10^{-11} S cm^{-1}, respectively, at room temperature, which could be negligible compared to the total conductivity.

Moreover, it demonstrated in general that the addition of ceramic nanofillers could improve the lithium transference number, due to surface interactions between fillers and polymer or salt[17,44]. It suggested that the interaction of ceramic nanofillers and polymer chain could promote local relaxation and segmental motion, which results in enhanced mobility of Li ions and an increased Li transference number[45]. It is also believed that by adding inorganic nanofillers, these interactions could dissociate $Li^+ClO_4^-$ ion pairs and increase the fraction of free Li ions, and subsequently enhance

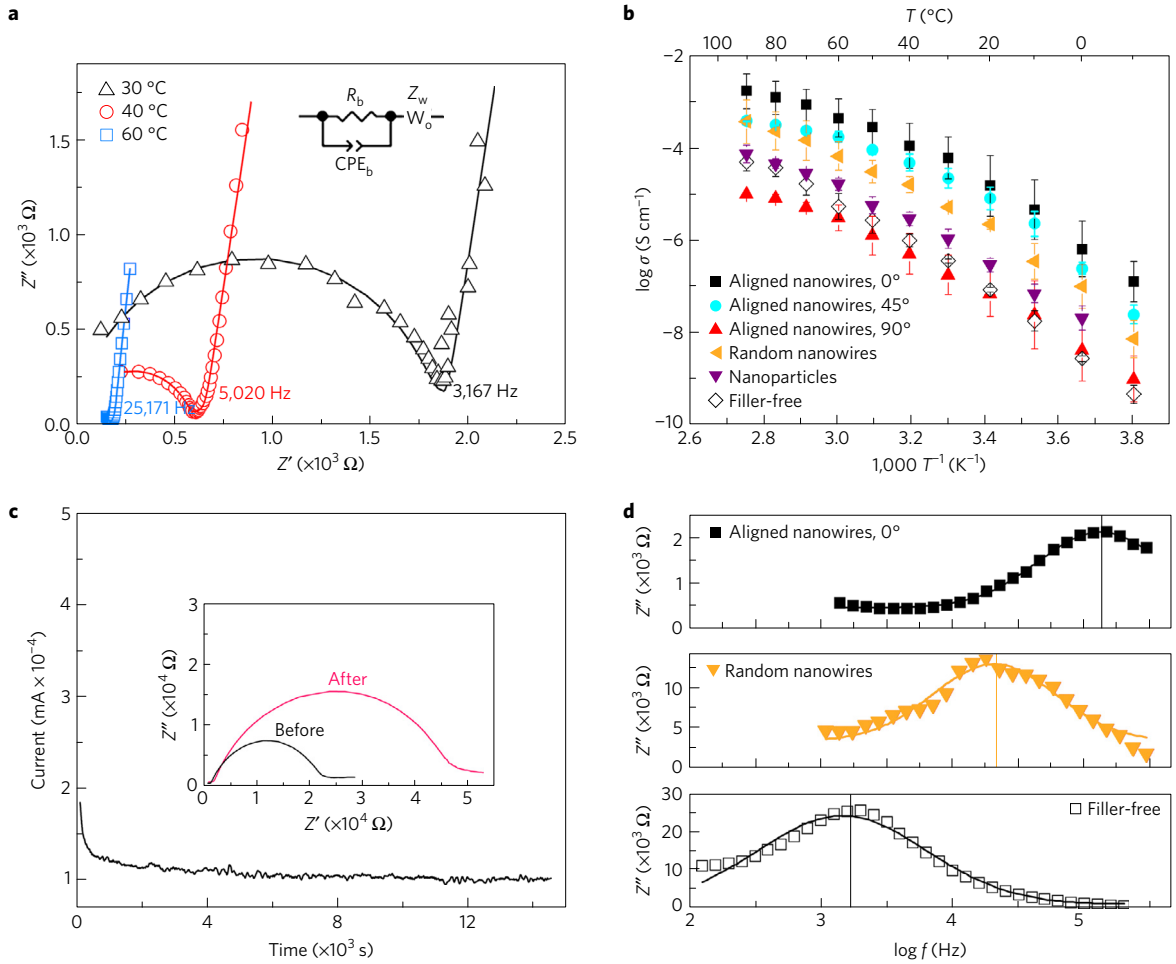

Figure 3 | Conductivity results for the composite polymer electrolyte with ceramic nanowires. a, Experimental and fitting (solid curves) impedance spectra for the composite polymer electrolyte with nanowires of 0° orientation measured at various temperatures. The inset shows the equivalent circuit. **b**, Arrhenius plots of the composite polymer electrolytes with aligned nanowire arrays at various orientations, together with the data for the composite electrolyte with randomly dispersed nanowires and the filler-free electrolyte. **c**, Variation of current with time during polarization of a Li/sample/Li configuration at an applied voltage of 10 mV; the inset figure shows the impedance spectra before and after polarization. **d**, Representative plots of imaginary impedance as a function of the log f (Debye plots) and fitting curves for the composite polymer electrolytes with aligned nanowires, for the composite electrolyte with random nanowires, and for the filler-free electrolyte, measuring at 40 °C. The vertical lines indicate the Debye peak positions.

the lithium transference number (t_+) (ref. 46). The t_+ values for SPEs were measured and calculated according to the equation[47]

$$t_+ = \frac{I_{ss}(\Delta V - I_0 R_0)}{I_0(\Delta V - I_{ss}R_{ss})} \quad (2)$$

where I_0 and I_{ss} are the initial and steady-state currents, ΔV is the potential applied across the cell, and R_0 and R_{ss} are the initial and steady-state resistance of the passivation layer. The variation of current with time and the impedance spectra before and after polarization for the composite polymer electrolyte with nanowires (3 wt%) are shown in Fig. 3c. Subsequently, t_+ for the polymer electrolyte was increased from 0.27 to 0.42 by adding LLTO nanowires. It should be noted that LLTO could react with Li metal at the interface between the polymer electrolyte and Li electrode, which may lead to an increased initial current I_0. Herein, the improvement conductivity for composite polymer electrolytes with nanowires due to Li ions has been clarified.

Li-ion transport mechanism

We plotted the imaginary impedance as a function of frequency (known as a Debye plot) and fitted it with a Lorentzian function (Fig. 3d), which indicates the relaxation time associated with ion hopping. The frequencies of the Debye peak maxima, a characteristic frequency of the conductivity relaxation, can be given by the reciprocal of the conductivity relaxation time (τ) or conductivity (σ) (ref. 48):

$$2\pi f_{max} = \omega = (\tau)^{-1} = \sigma(e_0\varepsilon')^{-1} \quad (3)$$

where ε' (real component of permittivity) is the frequency-independent permittivity, and e_0 is the permittivity of free space (8.854×10^{-14} F cm^{-1}). It can be seen that the peak position shifts toward higher frequencies on using aligned nanowires, implying a faster relaxation process. It can also be seen from Fig. 3b that, calculated from the slope of the temperature dependence of conductivity, the activation energies for the aligned-nanowire-filled electrolyte, random-nanowire-filled electrolyte and filler-free electrolyte are 0.77 ± 0.05, 0.84 ± 0.02 and 0.94 ± 0.04 eV, respectively. The composite polymer electrolytes have lower activation energies than the filler-free electrolyte, also implying a fast ion conduction pathway introduced by the nanowires[22,28,49].

The improvement of ionic conductivity when dispersing ceramic nanoparticles in SPE is believed to result from two possible mechanisms. Some researchers believe that ceramic particles can create an impediment to polymer crystallization[17]. The X-ray

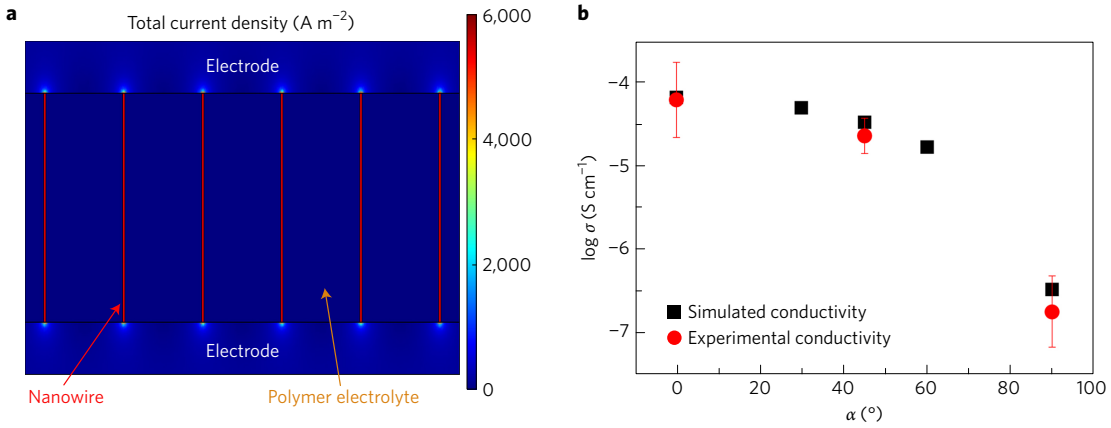

Figure 4 | Simulation analysis for the composite polymer electrolyte with aligned nanowires. a, Modelling of current densities for the composite polymer electrolyte with aligned nanowires (orientation angle is 0°). **b**, Conductivity versus angle for composite polymer electrolytes, showing the data for both simulated and experimental results.

diffraction patterns (Supplementary Figs 5 and 9) show a crystalline peak around 17°, corresponding to the (100) reflection of PAN, and a broad non-crystalline peak (20°–30°) (ref. 50). Also the sharp crystalline peaks corresponding to the $LiClO_4$ salt were found to be absent in the complexes, which indicates complete dissolution of lithium salts in the polymer. It also indicated from Supplementary Fig. 9 that dispersing 3 wt% nanowires into PAN has no obvious influence on PAN crystallinity. Also, from Supplementary Fig. 10 and Supplementary Table 1 (for details see Supplementary Note 3), the addition of 3 wt% nanowires has negligible influence on polymer crystallinity. Therefore, the conductivity enhancement by nanowires is not mainly attributed to reduced crystallization, in agreement with the reports[22,26,28,30,51–53]. They pointed out that the highly conductive surfaces of the inorganic fillers in the polymer could improve the ionic conductivity. Wieczorek *et al.*[25,26] applied the Lewis acid–base theory to explain the conductivity enhancement. It is proposed that a stronger affinity can be expected between ClO_4^- and acidic groups on the surface of nano-oxides, which helps to separate the $Li^+ClO_4^-$ ion pairs and increase the concentration of free Li ions that can move rapidly through the conductive pathways at the ceramic extended surface. Many reports have indicated rapid ion conduction at interfaces in heterostructured materials; however, the related reasons have been complex and highly debated. Maier *et al.*[54] demonstrated BaF_2/CaF_2 heterofilms and believed the space-charge effects were attributed to the observed anomalous transport properties. However, no observable effect of a space-charge layer on the ionic conductivity of LiI/Al_2O_3 interfaces was reported, and the nucleation and coalescence of epitaxial islands was the predominant factor[55].

To clarify the contribution of surface conduction, our previous work[56] revealed that the inorganic nanowires helped to dissociate ClO_4^- with Li^+ and then released more free Li ions, according to the FTIR spectra results. In addition, in the current study, we obtained N 1*s* XPS core level spectra (Supplementary Fig. 11, for details see Supplementary Note 4) and found that more free Li ions are released from bonding with N. Moreover, to further clarify the function of the Li-conductive nanowires in the composite electrolyte, it indicates that the inert ceramic nanowires (ZrO_2, 3 wt%) showed a smaller ionic conductivity enhancement compared with LLTO nanowires (Supplementary Fig. 12). Hence, the Li-vacancies are probably enriched and the Li-ion diffusion is not constrained to the surfaces of Li-conductive nanowires, thereby winning out over the inert nanowires. Hence, the surface region of LLTO nanowires with their high specific surface area and large aspect ratio provides a fast pathway for Li-ion diffusion to long distances without interruption.

Interestingly, and importantly, the composite polymer electrolyte with a well-oriented nanowire array could provide a possibility for calculation of the surface conductivity of the nanowire, which is beyond the ability of nanoparticles and randomly dispersed nanowires. On the basis of the data on nanowires with 0° alignment, the interface conductivity was deduced to be 1.26×10^{-2} S cm^{-1} (30 °C)—comparable to that of liquid electrolyte (for details see Supplementary Note 5). To confirm whether our calculated ionic conductivity is correct or not, 'Comsol Multiphysics' (Comsol) numerical analysis of the current distribution in composite polymer electrolytes with nanowires of various orientation angles (0°, 30°, 45°, 60° and 90°) has been carried out. We used the calculated surface conductivity of the nanowires at 0° as the starting parameters to predict the conduction behaviour at other angles. The detailed method and geometry are indicated in Supplementary Note 6. The colour map represents the current density, with the colour range adjusted for each case for composite polymer electrolytes with aligned nanowires of various orientations (Fig. 4a and Supplementary Fig. 13). The solid red line represents current flow for clear visualization of the current concentration. It can be seen that the current density is concentrated on the nanowires, indicating a higher ion-conducting behaviour than the polymer matrix. The simulated total conductivity with respect to the orientation of the nanowires is plotted in Fig. 4b and is in good agreement with experimental data. These results indicate the validity of our calculated surface conductivity data.

Conclusion

In summary, solid composite polymer electrolytes with well-aligned Li^+-conducting nanowires of various orientations have been studied, and they show exceedingly high ionic conductivities. Compared with the randomly dispersed nanowires, ten times enhancement in conductivity could be achieved for the well-aligned nanowires (6.05×10^{-5} S cm^{-1} at 30 °C). The surface conductivity of the nanowires is deduced to have a high value of ~1.26×10^{-2} S cm^{-1} at 30 °C, approaching the ion conduction in liquid electrolyte. We prove that the appreciable conductivity improvement is due to a fast ion conduction pathway without crossing junctions on the nanowire surfaces. In addition, the long-term conductivity stability for the polymer electrolytes is improved by adding the nanowires. The development of composite polymer electrolytes with aligned nanowires provides a promising approach for improving the ionic conductivity of solid electrolytes via a novel nano-architecture design. Moreover, the solid electrolyte with in-plane electrodes also has the capability to allow the development of micro-LIBs with improved storage capacity and power density.

Methods

Fabrication of interdigital electrode. The interdigital Pt electrodes were prepared by means of typical lithographic technology in the Stanford Nanofabrication Facility. Shipley 3612 Photoresist with a thickness of 1 μm was first spin-coated on quartz wafers followed by exposure and development. Prime refers to the use of HMDS as an adhesion promoter to help the resist stick to the wafer surface. Subsequently, a metal layer of Pt with a thickness of 100 nm was deposited on the wafer by means of an e-gun/beam evaporator (Kurt J. Lesker). The photoresist was then removed by sonication in acetone.

Synthesis of the ceramic nanowires. For preparation of the $Li_{0.33}La_{0.557}TiO_3$ (LLTO) nanowires, $LiNO_3$ (>99.99%), $La(NO_3)_3 \cdot 6H_2O$ (>99.99%) and $Ti(OC_4H_9)_4$ (>99.0%) of various corresponding molar mass were dissolved in dimethylformamide (DMF) with 20 vol.% acetic acid. An appropriate amount of polyvinylpyrrolidone (PVP, M_w = 130,000) was subsequently added. A transparent solution with a concentration of 12 wt% PVP was obtained by vigorous stirring. For the electrospinning procedure, the precursor solution was loaded into a 1 ml plastic capillary with a stainless-steel needle. A high voltage of 15 kV was applied by dipping a charged silver thread into the precursor solution. A grounded drum rotating at 6,000 r.p.m. was placed 15 cm beneath the needle to collect as-spun composite fibres. The interdigital Pt electrodes were placed on the collector at various angles. The as-spun wires were subsequently calcined at 800 °C for 2 h in air at a heating rate of 1 °C min^{-1}.

Synthesis of the composite polymer electrolyte with ceramic nanowires. For the composite electrolyte with random LLTO nanowire fillers, PAN and $LiClO_4$ (2:1 weight ratio) were first dissolved in DMF with a concentration of 10 wt% of PAN. LLTO nanowires with 3 wt% (total weight of PAN and $LiClO_4$) were then added in the above solution. The mixture was mechanically stirred at 80 °C for 5 h and then cast with a doctor blade on a glass plate. For the composite polymer electrolyte with well-aligned LLTO nanowires of various orientations, interdigital electrode was first fabricated by photolithography. The nanowires were prepared on the electrode by electrospinning and calcination, and then DMF solution containing PAN-$LiClO_4$ was coated on the nanowires. The LLTO nanoparticles were prepared by the sol–gel method. Finally, the as-obtained films were further dried in a high-vacuum oven at 80 °C for at least 48 h. They were then transferred into an argon-filled glove box (O_2 and H_2O at sub-ppm value, typically <0.6 ppm) and heated at 80 °C for at least 48 h before measurement to completely remove the solvent. All the SPEs, including the filler-free electrolyte and the composite electrolyte with nanowires, were prepared following the same procedures and drying temperature and time.

Characterization. Optical images were acquired by an Olympus BX51M microscope under normal white-light illumination. A differential scanning calorimeter (DSC, TA Instrument Q2000) was used to detect the crystallinity of the samples. Differential thermal analysis and thermogravimetry (DTA/TG, STA 449, Netzsch) were conducted on the samples under a simulated air atmosphere (20 vol.% O_2 in Ar, 99.99% pure gases from Airgas). The morphologies of samples were examined by scanning electron microscopy (SEM, FEI Nova NanoSEM 450) and transmission electron microscopy (TEM, FEI Tecnai G2 F20 X-TWIN microscope). X-ray photoelectron spectroscopy (XPS) data were taken from a PHI 5000 VersaProbe using an Al Kα (λ = 0.83 nm, $h\upsilon$ = 1,486.7 eV) X-ray source operated at 2 kV and 20 mA. The C 1*s* neutral peak at 284.6 eV was used as the reference to correct for the shift caused by surface-charging effects. Fourier transform infrared (FTIR) transmittance spectra were taken on a Bruker Vertex 70 FTIR spectrometer. The electrical conductivity investigated using a.c.-impedance spectroscopy were recorded by a Biologic VSP potentiostat over the frequency range from 0.10 Hz to 500 KHz. To carry out impedance spectroscopy of the nanowires without polymer coating, aligned as-spun fibres (same number, about 2,000, as that in the composite polymer electrolytes) were collected on the Pt interdigital electrode and then calcined at 800 °C. The lithium transference number for the solid polymer electrolyte was measured by chronoamperometry and a.c.-impedance spectra. Two lithium metal foils were used as the non-blocking electrodes. The electronic conductivity was measured by means of the Hebb–Wagner polarization technique. The solid polymer electrolyte was sandwiched between an ion-blocking electrode (Au) and a reversible electrode (Li). All the assemblies were carried out in a dry glove box filled with argon.

Received 29 March 2016; accepted 20 February 2017; published 3 April 2017

References

1. Quartarone, E. & Mustarelli, P. Electrolytes for solid-state lithium rechargeable batteries: recent advances and perspectives. *Chem. Soc. Rev.* **40**, 2525–2540 (2011).
2. Stephan, A. M. & Nahm, K. S. Review on composite polymer electrolytes for lithium batteries. *Polymer* **47**, 5952–5964 (2006).
3. Zheng, G. *et al.* Interconnected hollow carbon nanospheres for stable lithium metal anodes. *Nat. Nanotech.* **9**, 618–623 (2014).
4. Bouchet, R. *et al.* Single-ion BAB triblock copolymers as highly efficient electrolytes for lithium-metal batteries. *Nat. Mater.* **12**, 452–457 (2013).
5. Denoyel, R., Armand, M. & Fergus, J. W. Ceramic and polymeric solid electrolytes for lithium-ion batteries. *J. Power Sources* **195**, 4554–4569 (2010).
6. Armand, M. & Tarascon, J.-M. Building better batteries. *Nature* **451**, 652–657 (2008).
7. Aricò, A. S., Bruce, P., Scrosati, B., Tarascon, J.-M. & van Schalkwijk, W. Nanostructured materials for advanced energy conversion and storage devices. *Nat. Mater.* **4**, 366–377 (2005).
8. Cao, C., Li, Z., Wang, X. L., Zhao, X. & Han, W. Q. Recent advances in inorganic solid electrolytes for lithium batteries. *Front. Energy Res.* **2**, 25 (2014).
9. Oudenhoven, J. F. M., Baggetto, L. & Notten, P. H. L. All-solid-state lithium-ion microbatteries: a review of various three-dimensional concepts. *Adv. Energy Mater.* **1**, 10–33 (2011).
10. Agrawal, R. C. & Pandey, G. P. Solid polymer electrolytes: materials designing and all-solid-state battery applications: an overview. *J. Phys. D* **41**, 223001–223018 (2008).
11. Mizuno, F., Hayashi, A., Tadanaga, K. & Tatsumisago, M. New, highly ion-conductive crystals precipitated from Li_2S-P_2S_5 glasses. *Adv. Mater.* **17**, 918–921 (2005).
12. Minami, K., Hayashi, A. & Tatsumisago, M. Preparation and characterization of superionic conducting $Li_7P_3S_{11}$ crystal from glassy liquids. *J. Ceram. Soc. Jpn* **118**, 305–308 (2010).
13. Kamaya, N. *et al.* A lithium superionic conductor. A lithium superionic conductor. *Nat. Mater.* **10**, 682–686 (2011).
14. Kawai, H. & Kuwano, J. Lithium ion conductivity of a-site deficient perovskite solid solution $La_{0.67-x}Li_{3x}TiO_3$. *J. Electrochem. Soc.* **141**, L78–L79 (1994).
15. Zhu, Y., Zhang, Y. & Lu, L. Influence of crystallization temperature on ionic conductivity of lithium aluminum germanium phosphate glass-ceramic. *J. Power Sources* **290**, 123–129 (2015).
16. Wang, Y. & Zhong, W. H. Development of electrolytes towards achieving safe and high performance energy storage devices: a review. *ChemElectroChem* **2**, 22–36 (2015).
17. Croce, F., Appetecchi, G. B., Persi, L. & Scrosati, B. Nanocomposite polymer electrolytes for lithium batteries. *Nature* **394**, 456–458 (1998).
18. Hsu, C. Y. *et al.* High thermal and electrochemical stability of PVDF-graft-PAN copolymer hybrid PEO membrane for safety reinforced lithium-ion battery. *RSC Adv.* **6**, 18082–18088 (2016).
19. Wang, S. H. *et al.* Design of poly (acrylonitrile)-based gel electrolytes for high-performance lithium ion batteries. *ACS Appl. Mater. Inter.* **6**, 19360–19370 (2014).
20. Hong, H. *et al.* Studies on PAN-based lithium salt complex. *Electrochim. Acta* **37**, 1671–1673 (1992).
21. Qian, X. *et al.* Impedance study of $(PEO)_{10}LiClO_4$-Al_2O_3 composite polymer electrolyte with blocking electrodes. *Electrochim. Acta* **46**, 1829–1836 (2001).
22. Kim, J. W., Ji, K. S., Lee, J. P. & Park, J. W. Electrochemical characteristics of two types of PEO-based composite electrolyte with functional SiO_2. *J. Power Sources* **119–121**, 415–421 (2003).
23. Balazs, A. C., Emrick, T. & Russell, T. P. Nanoparticle polymer composites: where two small worlds meet. *Science* **314**, 1107–1110 (2006).
24. Choi, J. H. *et al.* Enhancement of ionic conductivity of composite membranes for all-solid-state lithium rechargeable batteries incorporating tetragonal $Li_7La_3Zr_2O_{12}$ into a polyethylene oxide matrix. *J. Power Sources* **274**, 458–463 (2015).
25. Wieczorek, W., Such, K., Wyciślik, H. & Płocharski, J. Modifications of crystalline structure of PEO polymer electrolytes with ceramic additives. *Solid State Ion.* **36**, 255–257 (1989).
26. Wieczorek, W., Florjancyk, Z. & Stevens, J. R. Composite polyether based solid electrolytes. *Electrochim. Acta* **40**, 2251–2258 (1995).
27. Hu, Y.-S. Getting solid. *Nat. Energy* **1**, 16042 (2016).
28. Weston, J. E. & Steele, B. C. H. Effects of inert fillers on the mechanical and electrochemical properties of lithium salt-poly (ethylene oxide) polymer electrolytes. *Solid State Ion.* **7**, 75–79 (1982).
29. Capuano, F., Croce, F. & Scrosati, B. Composite polymer electrolytes. *J. Electrochem. Soc.* **138**, 1918–1922 (1991).
30. Chiang, C. Y., Reddy, M. J. & Chu, P. P. Nano-tube TiO_2 composite PVdF/$LiPF_6$ solid membranes. *Solid State Ion.* **175**, 631–635 (2004).
31. Wagemaker, M. *et al.* Multiple Li positions inside oxygen octahedra in lithiated TiO_2 anatase. *J. Am. Chem. Soc.* **125**, 840–848 (2003).
32. Chu, P. P., Reddy, M. J. & Kao, H. M. Novel composite polymer electrolyte comprising mesoporous structured SiO_2 and PEO/Li. *Solid State Ion.* **156**, 141–153 (2003).

33. Croce, F. *et al.* Physical and chemical properties of nanocomposite polymer electrolytes. *J. Phys. Chem. B* **103**, 10632–10638 (1999).
34. Croce, F. *et al.* Role of the ceramic fillers in enhancing the transport properties of composite polymer electrolytes. *Electrochim. Acta* **46**, 2457–2461 (2001).
35. Quartarone, E., Mustarelli, P. & Magistris, A. PEO-based composite polymer electrolytes. *Solid State Ion.* **110**, 1–14 (1998).
36. Scrosati, B., Croce, F. & Persi, L. Impedance spectroscopy study of PEO-based nanocomposite polymer electrolytes. *J. Electrochem. Soc.* **147**, 1718–1721 (2000).
37. Liu, W. *et al.* Ionic conductivity enhancement of polymer electrolytes with ceramic nanowires fillers. *Nano Lett.* **15**, 2740–2745 (2015).
38. Cetiner, S. *et al.* Polymerization of pyrrole derivatives on polyacrylonitrile matrix, FTIR–ATR and dielectric spectroscopic characterization of composite thin films. *Synth. Met.* **160**, 1189–1196 (2010).
39. Phadke, M. A. *et al.* Poly (acrylonitrile) ultrafiltration membranes. I. Polymer-salt-solvent interactions. *J. Polymer Sci. B* **43**, 2061–2073 (2005).
40. Funke, K. Jump relaxation in solid electrolytes. *Prog. Solid State Chem.* **22**, 111–195 (1993).
41. Osman, Z. *et al.* AC ionic conductivity and DC polarization method of lithium ion transport in PMMA-$LiBF_4$ gel polymer electrolytes. *Results Phys.* **2**, 1–4 (2012).
42. Neudecker, B. J. & Weppner, W. Li_9SiAlO_8: a lithium ion electrolyte for voltages above 5.4 V. *J. Electrochem. Soc.* **143**, 2198–2203 (1996).
43. Kanno, R. *et al.* Synthesis of a new lithium ionic conductor, thio-LISICON–lithium germanium sulfide system. *Solid State Ion.* **130**, 97–104 (2000).
44. Scrosati, B., Croce, F. & Panero, S. Progress in lithium polymer battery R&D. *J. Power Sources* **100**, 93–100 (2001).
45. Lin, C. W. *et al.* Influence of TiO_2 nano-particles on the transport properties of composite polymer electrolyte for lithium-ion batteries. *J. Power Sources* **146**, 397–401 (2005).
46. Sun, H. Y. *et al.* Enhanced lithium-ion transport in PEO-based composite polymer electrolytes with ferroelectric $BaTiO_3$. *J. Electrochem. Soc.* **146**, 1672–1676 (1999).
47. Evans, J., Vincent, C. A. & Bruce, P. G. Electrochemical measurement of transference numbers in polymer electrolytes. *Polymer* **28**, 2324–2328 (1987).
48. Hodge, I. M., Ingram, M. D. & West, A. R. Impedance and modulus spectroscopy of polycrystalline solid electrolytes. *J. Electroanal. Chem.* **74**, 125–143 (1976).
49. Cantwell, P. R. *et al.* Grain boundary complexions. *Acta Mater.* **62**, 1–48 (2014).
50. Zhou, Z. *et al.* Development of carbon nanofibers from aligned electrospun polyacrylonitrile nanofiber bundles and characterization of their microstructural, electrical, and mechanical properties. *Polymer* **50**, 2999–3006 (2009).
51. Wieczorek, W., Stevens, J. R. & Florjańczyk, Z. Composite polyether based solid electrolytes. The Lewis acid-base approach. *Solid State Ion.* **85**, 67–72 (1996).
52. Nan, C. W., Fan, L., Lin, Y. & Cai, Q. Enhanced ionic conductivity of polymer electrolytes containing nanocomposite SiO_2 particles. *Phys. Rev. Lett.* **91**, 266104 (2003).
53. Gowneni, S., Ramanjaneyulu, K. & Basak, P. Polymer-nanocomposite brush-like architectures as an all-solid electrolyte matrix. *ACS Nano* **8**, 11409–11424 (2014).
54. Sata, N. *et al.* Mesoscopic fast ion conduction in nanometre-scale planar heterostructures. *Nature* **408**, 946–949 (2000).
55. Lubben, D. & Modine, F. A. Enhanced ionic conduction mechanisms at LiI/Al_2O_3 interfaces. *J. Appl. Phys.* **80**, 5150–5157 (1996).
56. Liu, W., Lin, D., Sun, J., Zhou, G. & Cui, Y. Improved lithium ionic conductivity in composite polymer electrolytes with oxide-ion conducting nanowires. *ACS Nano* **10**, 11407–11413 (2016).

Acknowledgements

This work is supported by Samsung Electronics.

Author contributions

W.L. and Y.C. conceived the experiment and carried out data analysis. W.L. performed materials fabrication and characterization. S.W.L. performed the numerical simulation. D.L., F.S. and S.W. assisted in experimental work. A.D.S. assisted in language editing. W.L. and Y.C. wrote the paper. All the authors discussed the results and commented on the manuscript.

Additional information

Supplementary information is available for this paper.

Reprints and permissions information is available at www.nature.com/reprints.

Correspondence and requests for materials should be addressed to Y.C.

How to cite this article: Liu, W. *et al.* Enhancing ionic conductivity in composite polymer electrolytes with well-aligned ceramic nanowires. *Nat. Energy* **2**, 17035 (2017).

Publisher's note: Springer Nature remains neutral with regard to jurisdictional claims in published maps and institutional affiliations.

Competing interests

The authors declare no competing financial interests.